Journal of the Korean Institute of Illuminating and Electrical Installation Engineers Vol. 17, No.4, pp. 74~80 July 2003 논문 17-4-11

침 대 중공평판전극에서 직류코로나 방전에 의한 이온풍 특성

(Characteristics of Ionic Wind in a DC Corona Discharge in Needle-to-punched plate Geometry)

이복희* · 길형준 · 엄주홍 · 안창환

(Bok-Hee Lee · Hyeong-Joon Kil · Ju-Hong Eom · Chang-Hwan Ahn)

요 약

직류 고전압이 침 대 평판전극에 인가된 불평등전장에서 코로나방전이 발생하게 되면 하전입자들의 이동에 의한 이온풍이 발생한다. 코로나 방전현상은 오존발생장치, 전기집진장치, 정전 냉각과 도색 등의 응용분야에서 다각도로 연구되어 왔으며, 최근 이온풍은 열전달장치, 공기순환장치 등에 이용되기도 한다. 본 연구에서는 침 대 중공평판전극에 직류 고전압을 인가하였을 때 발생하는 이온풍의 속도와 풍량의 제어 특성을 분석할 목적으로 인가전압, 중공의 크기, 전극간 거리의 변동에 따른 풍속의 변화를 측정하였다. 결과로서 이온풍에 의한 기류가 침전극으로부터 평판전극을 향하는 방향으로 발생하였으며, 중공평판전극의 후면의 100~200 [mm]지점에서 측정한 이온풍의 풍속은 인가전압에 따라 1~3[m/s]의 범위에서 증가하였다.

Abstract

Ionic wind is produced by a corona discharge when a DC high voltage is applied across the point-to-plane gap geometry. The corona discharge phenomena have been investigated in several beneficial application fields such as electrostatic cooling, ozone generation, electrostatic precipitation and electrostatic spraying. Recently ionic wind might be used in aerodynamic, for example, heat transfer, airflow modification, and etc. In this work, in order to analyze the control behavior of the velocity and amount of ionic wind produced by the positive DC corona discharges. The ionic wind velocity was measured as a function of the applied voltage, diameter of the punched hole on plate electrode and separation between the point-to-plate electrodes. As a results, the airflow is generated from the tip of needle to the plate electrode in the needle-to-punched-plate electrode systems. The ionic wind velocity is linearly increased with an increase in applied voltage and ranges from 1 to 3 m/sec at the locations of 100-200 mm from the punched-plate

Key Words : Ionic wind, Corona discharge, Aerodynamic system, Airflow modification

* 주저자 : 인하대학교 전자전기공학부
차세대 고전압전력기술연구센터 교수
Tel : 032-860-7398, Fax : 032-863-5822
E-mail : bhlee@inha.ac.kr
접수일자 : 2003년 2월 19일
1차심사 : 200 년 2월 28일
심사완료 : 200 년 4월 22일

1. Introduction

Corona discharge is the partial discharges that occur when a sharp needle is exposed to highly enhanced electric fields. The electrical effects of corona discharge are employed in a variety of technologies such as electrostatic precipitators, ozone generators, air cleaners, and so on. When a free electron is driven by the electric field toward the anode, it produces an electron avalanche. The cloud of positive ions produced at the avalanche head near the anode forms an eventual extension to the anode. Secondary generations of avalanche get directed to the anode and to these dense clouds of positive ions, and this process is repeated[1]. The electrons tend to follow the ions to neutralize the charge separation. Also corona discharge induces ion movement from the tip of needle to plate direction called electro-convection or ionic wind (also termed electric wind or corona wind). Ionic wind is a secondary effect of the interaction of corona discharge with its medium and this electrical effect has been widely studied in the needle and plate gap geometry[2-4]. Also the typical airflow visualization ionic wind patterns in the needle-plate electrodes arrangement by using the smoke wire method have presented in the literature[5]. Unfortunately, the electrical effect and phenomenon of ionic wind in corona discharge were not understood completely, many questions regarding theoretical formulations and behaviors of ionic wind movements have remained unanswered.

This work is aimed to analyze the effects of gap geometry and applied electric field on ionic wind velocity. The needle-to-punched plate configuration was selected for a detailed investigation of ionic wind generation, since it yields a reasonably high ionic wind velocity with a compact size and well-understood theory of operation[4],[6]. Also the needle-to-punched-plate electrode system allows the flow of ionic wind to pass through it when the corona discharge is occurred by the DC voltage at the tip of needle electrode. The ionic wind velocity at the back of the punched-plate electrode was measured as a function of the applied voltages and electrode configurations, separation between the needle-to-punched plate electrodes, and the experimental results were discussed.

2. Experimental Procedure

Figure 1 illustrates a circuit diagram of the DC high voltage generator used in this work. The rated voltage of this generator is 100[kV]. The capacitors are charged during a half-cycle of the secondary voltage of transformer, and the output voltage of DC high voltage generator is 2 times the peak value of the secondary voltage of transformer. Figure 2 shows the configurations of electrode systems and the tip of needle was arranged on the axis of the center of the punched plate.

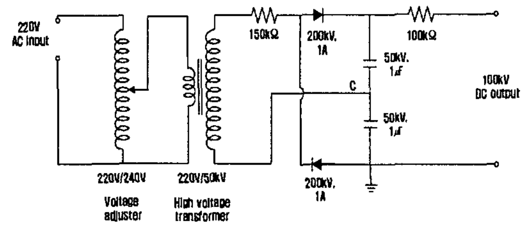

Fig.1. Circuit diagram of the DC high voltage generator

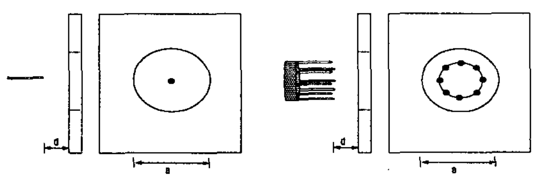

(a) Front and side views of the needle-to-punched plate

(b) Front and side views of the 8 needles-to-punched plate

Fig. 2. Configurations of the needle-to-punched plate electrode systems

Two types of electrode systems, for example, a needle-to-punched plate electrode system and 8 needles-to-punched plate electrode systems, were used in this experiment, and the positive polarity of DC voltage is applied at the needle electrode. The ionic wind velocity is controlled by the diameter of punched hole on the plate electrode, the distance between the needle and plate electrode, and the amplitude of applied voltage. The plate electrode was made of aluminum. The needle electrode was made of steel, whose diameter was 2[mm]. Measurements of the ionic wind velocity were made by using the thermal anemometry with temperature compensator because of the incompatibility of metallic probes in strong electric fields. The experiments were conducted in DC voltage ranges from 6 to 55 kilovolts as a parameter of the separation between the needle and plate electrodes.

3. Results and Discussion

3.1 Ionic wind velocity in a needle-to-punched plate electrodes

When a DC corona discharge is occurred in inhomogeneous fields, ions move from the injection electrode to the collection electrode direction, and air molecules around the ions were forced to move with following the ions. That airflow caused by ions moving is called ionic wind. It is considered that the ionic wind could be effected by sound wave[7]. The corona discharge process is markedly dependent on the geometry of the electrodes and on the polarity of the applied voltage.

In this work, characteristics of ionic wind in a DC corona discharge induced by application of a high positive potential at a needle electrode in the needle-to-punched plate electrode systems were experimentally investigated. Corona discharge is the media for carrying the electric charges from the ionization zone to air molecules and then into the surrounding space. Ions, which drift from the needle electrode to the plate one, transfer momentum by collision with the neutral particles and induce their movement. In the presence of positive corona, the needle electrode attracts electrons from the nearby air molecules, and positive ions recede from the needle electrode. Ionization increases drastically with increasing the applied electric field strength, and ionic wind velocity is linearly increased with ion flow. The factors of effecting on the ionic wind velocity include the polarity of applied voltage , the gap geometry such as shape of the needle and plate electrodes, the number of needle electrodes, the separation across needle-to-plate electrodes, and so on.

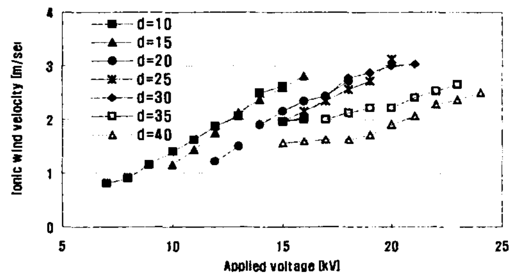

(a) Ionic wind velocity at the location of 100[mm] from the punched-plate

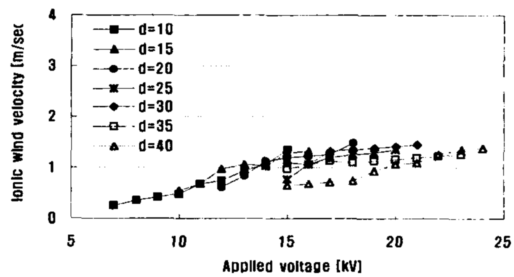

(b) Ionic wind velocity at the location of 200[mm] from the punched-plate

Fig. 3. Ionic wind velocity in a needle-to-plate with the punched hole of 20mm in diameter.

In order to detect the ionic wind velocity at the backside of the punched plate electrode, the electrode systems of the needle-to-plate with a punched hole were used. An anemometer was placed behind the punched plate electrode. Ionic wind velocities were measured at the location of

100 and 200[mm] from the punched-plate with the hole of 20[mm] as a parameter of the separation between the needle and plate electrodes.

The ionic wind is flowed from the needle electrode to the plate electrode and passes through the hole on the plate electrode. Because the hole on the plate electrode is a round shape, the torch shape luminous part of corona discharge is elongated toward the center of the hole on the plate electrode as the applied voltage is increased. The corona discharge is concentrated in visible spot at the tip of needle electrode, and the ionic wind velocities in the voltage ranges of 15 and 25 kilovolts are linearly increased as shown in Fig. 3. If the applied voltage is raised up to the upper limit at each gap separation, the inter-electrode space sparks over.

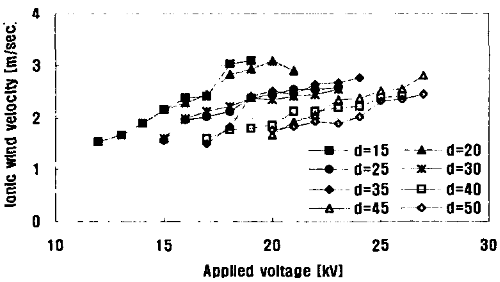

(a) Ionic wind velocity at the location of 100[mm] from the plate with punched hole

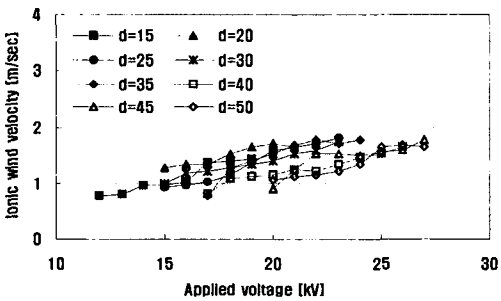

(b) Ionic wind velocity at the location of 200[mm] from the plate with punched hole

Fig. 4. Ionic wind velocity in a needle-to-plate with the punched hole of 40mm in diameter.

The applied electric field provides the driving force for movement of charged particles toward the low potential electrode. The ionic wind velocity is linearly proportional to the amplitude of applied voltages before corona is arrived at the state of burst-pulse streamers. The maximum ionic wind velocities were nearly independent of the separation between the needle-to-punched plate electrodes. The ionic wind occurs from the inception voltage of corona discharge, and airflow is accelerated from the tip of needle electrode toward the punched plate electrode. Thus the curves of the ionic wind velocity versus applied voltage are shifted to the zone of high voltage with the separation between the needle-to-punched plate electrodes. In the case that the diameter of punched hole is 20[mm], the maximum ionic wind velocities were 3.2 and 1.5[m/sec] at the location of 100 and 200[mm] from the punched-plate, respectively. When the anemometer moved from the location of 100[mm] to the location of 200[mm], the ionic wind velocity was decreased by 50%. The results obtained in the needle-to-plate electrodes whose punched holes are 40 and 60[mm] in diameter were shown in Figs. 4 and 5, respectively.

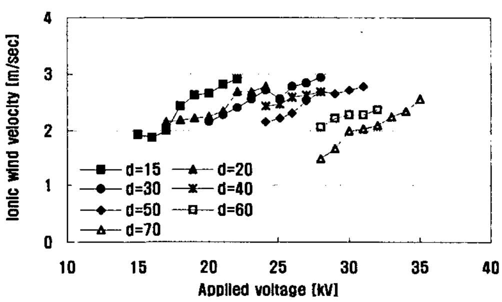

(a) Ionic wind velocity at the location of 100[mm] from the punched-plate

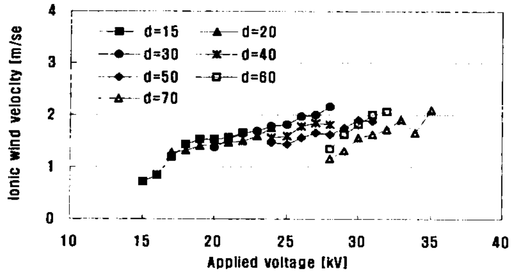

(b) Ionic wind velocity at the location of 200[mm] from the plate with punched hole

Fig. 5. Ionic wind velocities in a needle-to-plate with the punched hole of 60[mm] in diameter

The maximum ionic wind velocities were about 3[m/sec] at the location of 100[mm] from the punched plate and are nearly same with the data in the punched hole of 20[mm] in diameter. The ionic wind velocity is decreased with an increase in distance from the punched plate to the detecting point, and the ionic wind velocity at the location of 200[mm] is approximately 70% of the data at the location of 100[mm] when the applied voltage is consistent with the same value.

3.2 Ionic wind velocities in 8 needles-to-punched plate electrodes

The ionic wind velocity is strongly dependent on the distance between the center of punched-plate to the measuring point in single needle-to-punched plate. The amount and reaching range of ionic wind are small and short, respectively. Thus in order to improve the weak points in the single needle-to-punched plate, the ionic wind velocities in 8 needles-to-punched plate electrode systems with the hole of 80, 100 and 120[mm] were measured. The results were similar tendency to the case of ionic wind in a needle-to-plate electrodes geometry as illustrated in Figs. 6 and 8.

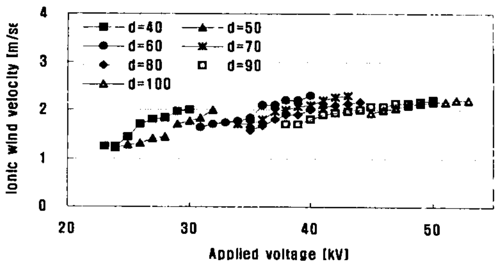

(a) Ionic wind velocity at the location of 100[mm] from the punched-plate

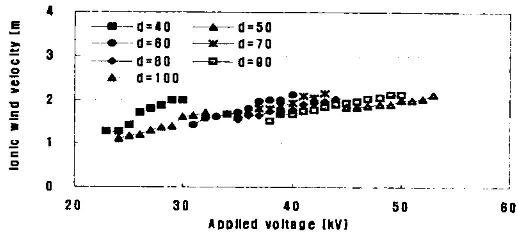

(b) Ionic wind velocity at the location of 200[mm] from the plate with punched hole

Fig. 6. Ionic wind velocities in 8 needles-to-plate with the punched hole of 80[mm] in diameter

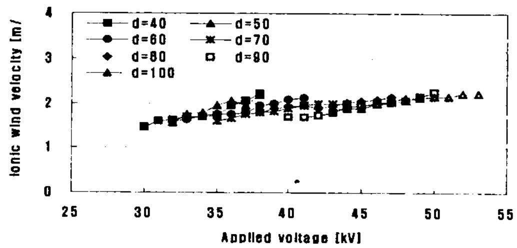

(a) Ionic wind velocity at the location of 100[mm] from the punched-plate

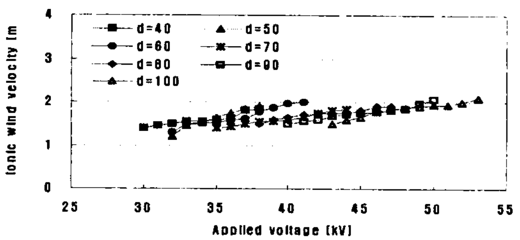

(b) Ionic wind velocity at the location of 200[mm] from the punched-plate

Fig. 6. Ionic wind velocity in 8 needles-to-plate with the punched hole of 100[mm] in diameter

The maximum ionic wind velocity was approximately 2.2[m/sec] irrespective of the diameter of punched hole on the plate electrode. Also the ionic wind velocity at the location of 100[mm] is almost same with that at the location of 200[mm]. These results showed that the ionic wind velocity in the 8 needles-to-plate with the large diameter of punched hole is stable in the wide zone behind the punched plate compared to the single needle-to-plate electrodes. The maximum ionic wind velocity is lower than the results obtained in a single needle-to-punched plate, but the airflow gain in quantity.

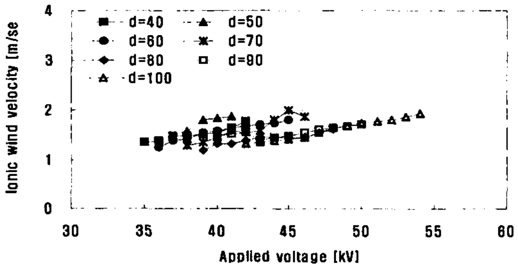

(a) Ionic wind velocity at the location of 100[mm] from the punched-plate

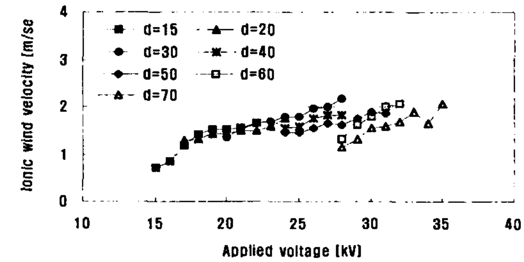

(b) Ionic wind velocity at the location of 200[mm] from the punched-plate

Fig. 8. Ionic wind velocity in 8 needles-to-plate with the punched hole of 120[mm] in diameter

3.3 Ionic wind velocity in needles-to-cylindrical electrode system

In order to improve the amount and concentration of ionic wind, the electrode system of 8 needles-to-cylinder connected in series to 4 needles-to-cylinder was made as shown in Fig. 9. Here the cylinder is 80[mm] in diameter and 70[mm] in length. The distance from the tip of point to the center of cylinder in second stage electrode system was fixed with 50[mm]. This series connection of the two needles-to-cylinder electrode systems is an experimentally convenient design in which aerodynamic effects are sufficiently allowed to the ionic wind. The ionic wind velocity versus the applied voltage curves were plotted as a parameter of the distance from the tip of needle electrode to the center of cylinder in first stage electrode system as shown in Fig. 10.

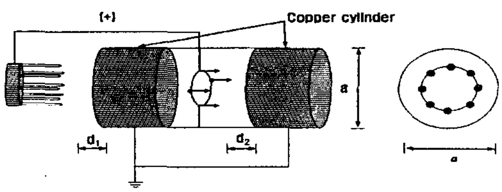

Fig. 9. Configuration of multistage needles-to-cylindrical electrode system

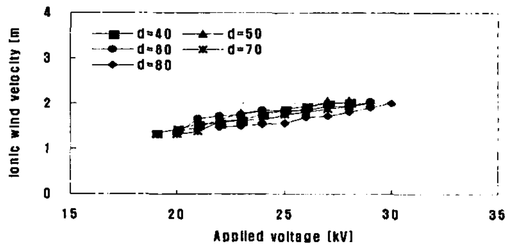

(a) Ionic wind velocity at the location of 100[mm] from the cylinder

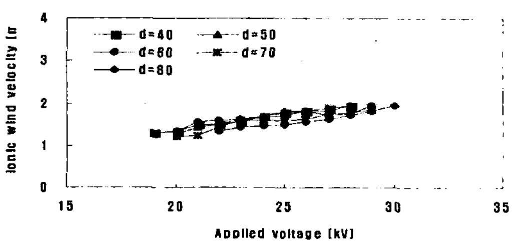

(b) Ionic wind velocity at the location of 200[mm] from the cylinder

Fig. 10. Ionic wind velocity in the multistage needles-to-cylinder electrode system

The maximum ionic wind velocity was 2[m/sec] that is about the same as the data in the 8 needles-to-plate with the punched hole of 80[mm] in diameter. The ionic wind velocity versus the applied voltage curves at the location of 100[mm] from the cylinder is nearly overlapped, and the curves at the location of 200[mm] and is independent of the distance from the tip of point to the center of cylinder in the first stage electrode systems. It was found that the amount of ionic airflow has increased and the directional movement of ionic wind has markedly improved in multiple needles-to-cylinder electrode systems

4. Conclusion

This paper has dealt with the control behaviors of the airflow of ionic wind due to the electrical discharge in strong inhomogeneous fields. The ionic wind velocity induced by the positive DC corona discharge was measured in the needle-to-plate with punched hole gap geometry, and the results could be summarized as follows;

The ionic wind velocity is increased up to about 3.2[m/sec] with an increase in applied voltage in a needle-to-plate with punched hole electrode system. The maximum ionic wind velocity was slightly decreased in multiple needles-to-plate and multiple needles-to-cylinder electrode systems, but the amount and directional movement of ionic wind are significantly improved. As a consequence, the ionic wind velocity can linearly be controlled over the range of 1-2[m/sec] in multiple needles-to-cylinder gap geometry, this approach provides a steady uniform flow of ionic wind and would effectively be used in aerodynamic systems.

References

[1] M. Abdel-Salam, H. Anis, A. Ei-Morshedy and R. Radwan, High-Voltage Engineering, Marcel Dekker, Inc. 2nd edition, pp.149~184, 2000.

[2] G. A. Kallio and D. E. Stock "Flow visualization inside a wire-plate electrostatic precipitator" IEEE Trans. on Industry App. Vol. 26, No. 3, pp.503~513, 1990.

[3] Y. Kagiwada, T. Hirata, T Nakane, T. Otsuka and K. Seya, "Behavior of ionic wind of corona discharge in ultrasonic field", IEEE 1991 Ultrasonic Symposium, pp.1015~1018, 1991.

[4] R. Honma and R. Ohyama, "Experimental study on Ionic wind measurement of an electrohydro-dynamically induced gas-liquid two-phase flow field by particle image velocimetry", Proc. Conf. on Elec. Insulation and Dielectric Phenomena, Vol.1, pp.81~84, 2000.

[5] R. Honma and R. Ohyama, "Experimental Study on Ionic Wind Measurement of an Electrohydrodynamically Induced Gas- Liquid Two-Phase Flow Field by Particle Image Velocimetry", Proc. IEEE Conference on Electrical Insulation and Dielectric Phenomena, pp.81~84, 2000.

[6] L. Leger, E. Moreau, G Touchard, "Control of Low Velocity Airflow along a Flat Plate with a DC electrical discharge", IEEE Conf. Record of 2001, Vol.3, pp.1536~1542, 2001.

[7] Y. Kagiwada, T. Hirata, T. Nakane, T. Otsuka, and K. Seya, "Behavior of Ionic Wind of Corona Discharge in Ultrasonic Field", Proc. IEEE Ultrasonics Symposium, pp.1015~1018, 1991.

◇저자소개◇

이복희 (李福熙)
1954년 6월 29일생. 1980년 2월 인하대 공대 전기공학과 졸업. 1987년 동 대학원 전기공학과 졸업(박사). 1988~89년 동경대학 생산기술연구소 객원연구원. 1995년 호주 Queensland대학 방문교수. 1999년 Cincinnati대학 방문교수. 현재 인하대 공대 전자전기공학부 교수. e-mail : bhlee@inha.ac.kr

길형준 (吉亨准)
1969년 8월 27일생. 1997년 2월 인하대 공대전기공학과 졸업. 1999년 2월 인하대 대학원졸업(석사). 현재 한국전기안전공사 부설 전기안전연구원 근무. 인하대 대학원 전기공학과 박사과정.
e-mail : g2001100@inhavision.inha.ac.kr

엄주홍 (嚴柱弘)
1972년 9월 5일생. 1998년 2월 인하대 공대 전기공학과 졸업. 2000년 2월 인하대 대학원 졸업(석사). 2002년 현재 인하대 대학원 전기공학과 박사과정.
e-mail : fa523@hanmir.com

안창환 (安昌煥)
1959년 11월 4일생. 1983년 2월 원광대학교 전기공학과 졸업. 1991년 2월 인하대 대학원 전기공학과 졸업(석사). 1999년 8월 인하대 대학원 전기공학과 졸업(박사). 현재 한국전력.
e-mail : Chahn@kepco.co.kr